Supplementary Information (SI) for Inorganic Chemistry Frontiers.

Supporting Information

Unveiling the unique mechanism of the UV-sensitive phosphonate-based metal-organic frameworks

Wenzhuo Tan,[ab] Li Xu,[ab] Ziwei Liu,[ab] Jihu Su,[c] and Tao Zheng *[ab]

[a.] *School of Materials Science and Engineering, Northwestern Polytechnical University, Xi'an 710072, P. R. China. E-mail: zhengtao@nwpu.edu.cn*
[b.] *Institute of Clean Energy, Yangtze River Delta Research Institute, Northwestern Polytechnical University, Suzhou 215400, P. R. China.*
[c.] *Hefei National Laboratory for Physical Sciences at Microscale and Department of Modern Physics, University of Science and Technology of China, Hefei 230026, P. R. China*

Contents

1. Results and Discussion

1.1 The Phosphonate Ligand and the Guest Molecules

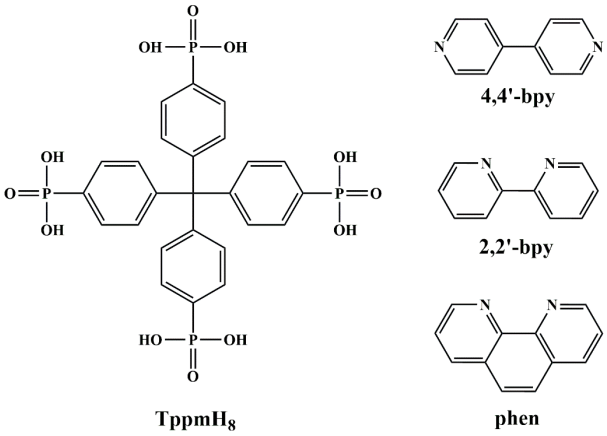

Figure S1. The $TppmH_8$ ligand and guest molecules.

1.2 Crystal Data and Structures

Table S1. Crystal data and refinement details for **UPF-112**, **UPF-113** and **UPF-114**.

	UPF-112	**UPF-113**	**UPF-114**
Formula	$C_{40}H_{40}O_{17}P_4N_3U$	$C_{35}H_{32}O_{18}P_4U_2N_2$	$C_{74}H_{58}O_{30}P_8U_3N_4$
M	1196.68	1368.58	2445.14
CCDC No.	2295557	2295555	2295556
Crystal system	Monoclinic	Triclinic	Monoclinic
Space group	$P2_1/n$	$P\bar{1}$	$C2/c$
a / Å	13.0819(13)	10.7280(12)	21.053(6)
b / Å	24.404(2)	15.0760(16)	14.058(4)
c / Å	13.3433(12)	15.4046(18)	28.441(8)
α / deg	90	61.166(5)	90.000
β / deg	109.386(3)	71.045(5)	111.043(8)
γ / deg	90	80.722(5)	90.000
V /Å3	4018.3(6)	2064.2(4)	7856(4)
Z	4	2	4
ρ_{calcd} / g cm^{-3}	1.908	2.168	2.062
F (000)	2252	1258	4640
μ(Mo Kα) /mm^{-1}	4.277	8.068	6.421
GOF on F^2	1.030	1.092	1.021
R_1[a], wR_2[b] [I>2σ(I)]	0.0315, 0.0896	0.1013, 0.2887	0.0374, 0.0870
$(\Delta\rho)_{max}$, $(\Delta\rho)_{min}$ / eÅ^{-3}	2.33, -0.9	11.78, -5.58	2.22, -1.12
porosity	36%	30%	27%

[a.] $R_1 = \Sigma||F_o| - |F_c|| / \Sigma|F_o|$. [b.] $wR_2 = [\Sigma w(Fo^2 - Fc^2)^2 / \Sigma w(Fo^2)^2]^{1/2}$

Table S2. Bond lengths of **UPF-112**.

Bond	Lengths [Å]	Bond	Lengths [Å]
U1=O13	1.771(3)	P2-O4 ^{HP}	1.541(3)
U1=O14	1.773(3)	P2-O5 ^{HP}	1.546(4)
U1-O1	2.354(3)	P2=O6	1.484(3)
U1-O12A	2.354(3)	P3-O7 ^{HP}	1.556(3)
U1-O6B	2.361(3)	P3-O8 ^{HP}	1.516(3)
U1-O9C	2.371(3)	P3-O9	1.506(3)
U1-O1w	2.594(4)	P4-O10	1.549(4)
P1-O1	1.501(3)	P4-O11	1.519(4)
P1=O2	1.496(3)	P4-O12	1.515(3)
P1-O3^{P}	1.582(4)		

Symmetric codes for **UPF-112**: A: 1/2+x, 3/2-y, 1/2+z; B: 3/2-x, 1/2+y, 3/2-z; C: x, y, 1+z. ^{P}: the oxygen atom is protonated. ^{HP}: the oxygen atom is half protonated.

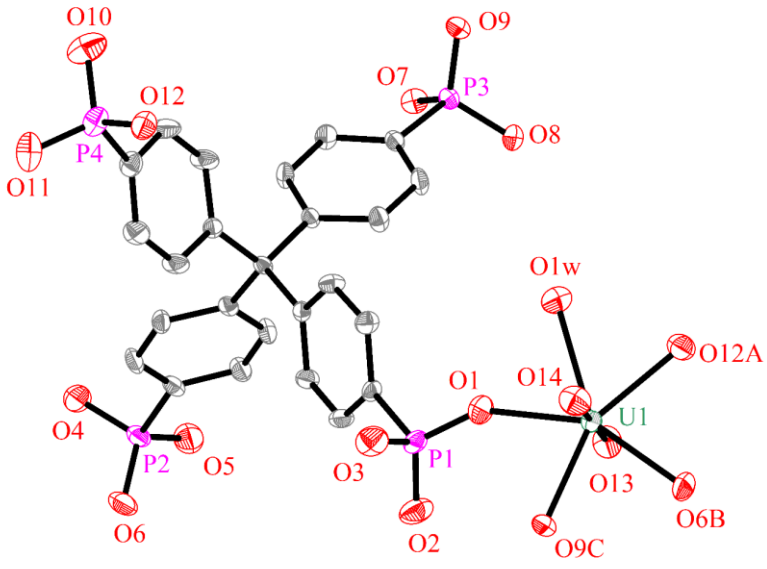

Figure S2. Asymmetric building unit of **UPF-112** with atomic labeling scheme at 50% probability. All hydrogen atoms and 4,4'-bpy molecules are omitted for clarity.

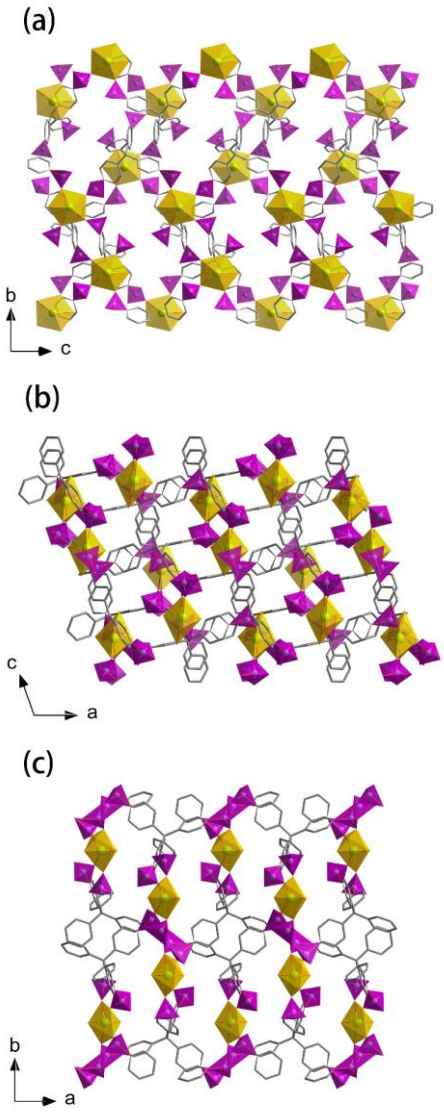

Figure S3. Crystal framework structures of **UPF-112** (a, b, and c), viewed along *a*, *b*, and *c* axis, respectively. UO_7 is represented by the yellow pentagonal bipyramid, while -CPO_3 is represented as a purple tetrahedron, and the guest molecules are omitted for clarity.

UPF-112 crystallizes in the monoclinic space group $P2_1/n$. The asymmetric unit contains one UO_2^{2+} cation, one $TppmH_8$, one and a half 4,4'-bpy, one coordinated water molecule, and two lattice water molecules (Fig. S2). UO_2^{2+} cation adopts a pentagonal bipyramid coordination geometry, forming UO_7 units. O1, O1w, O12A, O6B, and O9C are in the equatorial plane (Figs. S3a-S3c). The bond lengths of U=O and U-O are in the range of 1.771(3)-1.773(3) Å and 2.354(3)-2.371(3) Å, respectively. The bond length of U1-O1w is 2.594(4) Å, which is longer than other bonds between uranium atoms and coordinated water molecules. UO_7 units act as zero-dimensional secondary building units (0D-SBU) connecting four $TppmH_8$ ligands to give porous 3D frameworks with 4,4'-bpy molecules filled inside (Figs. S3a and S3b). 4,4'-bpy molecules are part or fully protonated to balance the charge, forming hydrogen bonds with the phosphonate groups in the framework structure. The P-O bond lengths in the range of 1.496(3)-1.516(3) Å (1.496(3) Å of P1-O2, 1.484(3) Å of P2-O6, 1.506(3) Å of P3-O9, 1.515(3) Å of P4-O12) are assigned to P=O groups. The bond length of P1-O3, P2-O4, P2-O5, P3-O7, and P4-O10 is 1.582(4) Å, 1.541(3) Å, 1.546(4) Å, 1.556(3) Å, and 1.549(4) Å, respectively, showing that O3 is fully protonated and the other oxygen atoms are half protonated (Table S2).

Table S3. Bond lengths of **UPF-113**.

Bond	Lengths [Å]	Bond	Lengths [Å]
U1=O13	1.783(15)	U3-O7E	2.338(18)
U1=O13J	1.783(16)	U3-O10	2.40(2)
U1-O1	2.242(17)	U3-O1w	2.54(2)
U1-O1J	2.242(17)	P1-O1	1.502(18)
U1-O6A	2.308(17)	P1-O2	1.534(19)
U1-06K	2.308(17)	P1-O3	1.527(17)
U2=O14	1.797(19)	P2-O4	1.50(2)
U2=O14I	1.797(19)	P2-O5 ^{P}	1.56(2)
U2-O2B	2.180(18)	P2-O6	1.51(2)
U2-O2G	2.180(18)	P3-O7	1.485(18)
U2-O4	2.24(2)	P3-O9	1.517(16)
U2-O4I	2.24(2)	P3-O8 ^{P}	1.590(18)
U3=O15	1.77(2)	P4-O10	1.508(17)
U3=O16	1.79(2)	P4-O11 ^{HP}	1.541(18)
U3-O3C	2.312(16)	P4-O12 ^{HP}	1.518(17)
U3-O9D	2.32(2)		

Symmetric codes for **UPF-113**: A: 2-x, 1-y, 1-z; B: x, 1+y, z; C: x, y, 1+z; D: 1-x, 1-y, 2-z; E: 1+x, y, z; G: 1-x, 1-y, 1-z; I: 1-x, 2-y, 1-z; J: 2-x, -y, 1-z; K: x, -1+y, z. ^{P}: the oxygen atom is protonated. ^{HP}: the oxygen atom is half protonated.

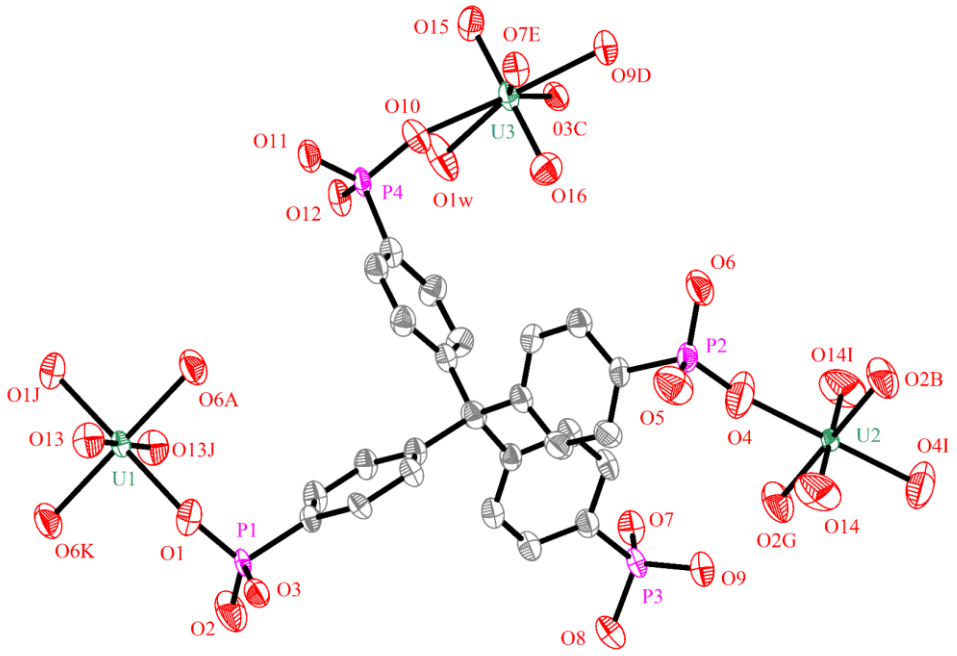

Figure S4. Asymmetric building unit of **UPF-113** with atomic labelling scheme at 50% probability. All hydrogen atoms and 2,2'-bpy molecules are omitted for clarity.

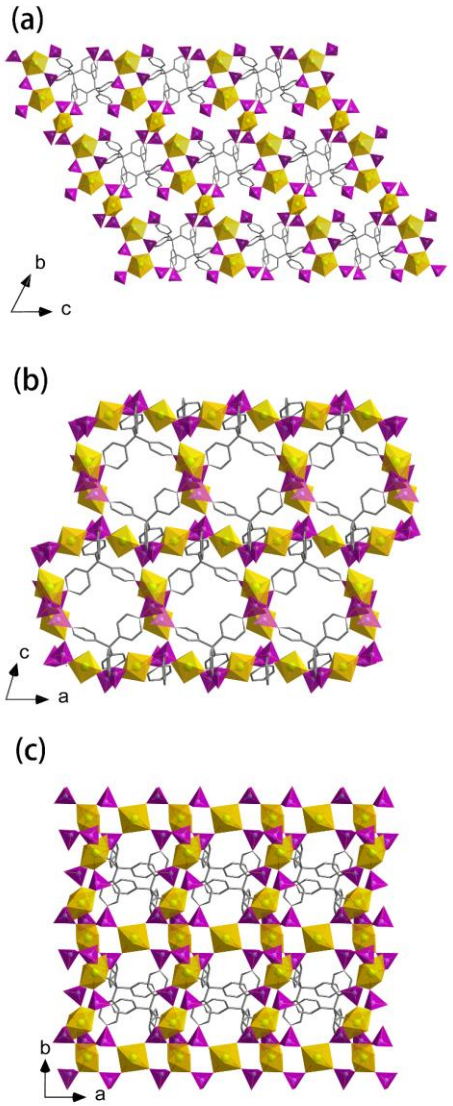

Figure S5. Crystal framework structures of **UPF-113** (a, b, and c), viewed along *a*, *b*, and *c* axis, respectively. UO_6 and UO_7 are represented by the yellow tetragonal bipyramid and pentagonal bipyramid, while -CPO_3 is represented as a purple tetrahedron, and the guest molecules are omitted for clarity.

UPF-113 crystallizes in the triclinic space group $P\bar{1}$. The asymmetric unit contains one and two half UO_2^{2+} cations, which are crystallography different, one $TppmH_8$ ligand, two half 2,2'-bpy molecules, one coordinated water molecule, and one lattice water molecule (Fig. S4†). As presented in Figure 1d-1f, UO_2^{2+} cations adopt tetragonal and pentagonal bipyramid coordination geometry, respectively. The bond lengths of U=O and U-O are in the range of 1.77(2)-1.797(2) Å and 2.18(2)-2.40(2) Å, respectively. And the bond length of U3-O1w is 2.54(2) Å. For U1 and U2 in UO_6 units, four oxygen atoms located at the equatorial plane are provided by four $TppmH_8$ ligands and 1D- SBUs are achieved along the *a* axis consisting of U1 and U2 in UO_6 units arranged alternatively. For U3, O3C, O9D, O7E, O10, and O1w are located in the equatorial plane, forming the UO_7 cluster. UO_7 units are connected by $TppmH_8$ ligands, giving porous layers, which are further linked by 1D-SBUs to construct the final 3D structure. The bond lengths of P2-O5, P3-O8, P4-O11, and P4-O12 are in the range of 1.52(2)-1.59(2) Å, showing that O5 is protonated and the other oxygen atoms are half protonated (Table S3†).

Table S4. Bond lengths of **UPF-114**.

Bond	Lengths [Å]	Bond	Lengths [Å]
U1=O13	1.760(4)	P1-O2	1.497(4)
U1=O13E	1.761(4)	P1-O3 ^{P}	1.549(4)
U1-O2	2.278(4)	P2-O4	1.515(4)
U1-O2E	2.278(4)	P2-O5 ^{P}	1.567(4)
U1-O10A	2.294(4)	P2-O6	1.502(4)
U1-O10F	2.294(4)	P3-O7	1.494(4)
U2=O15	1.777(4)	P3-O8	1.511(4)
U2=O14	1.788(4)	P3-O9 ^{P}	1.551(4)
U2-O4B	2.243(4)	P4-O10	1.503(4)
U2-O7C	2.256(4)	P4-O11	1.496(4)
U2-O8D	2.295(4)	P4-O12 ^{P}	1.578(4)
P1-O1	1.498(4)		

Symmetric codes for **UPF-114** : A: x, -1+y, z; B: 1/2-x, -1/2-y ,-z; C: 1/2-x, -1/2+y, -1/2-z; D: x, -1-y, 1/2+z; E: -x, y, -1/2-z; F: -x, -1+y, -1/2-z. ^{P}: the oxygen atom is protonated. ^{HP}: the oxygen atom is half protonated.

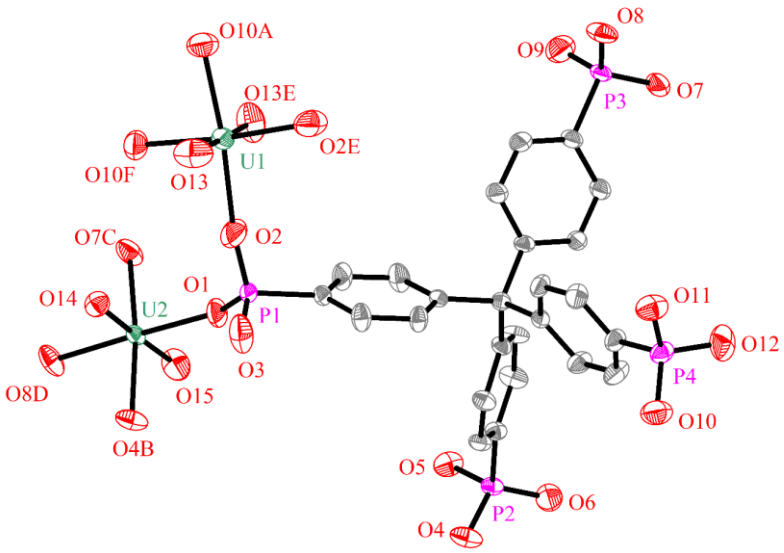

Figure S6. Asymmetric building unit of **UPF-114** with atomic labeling scheme at 50% probability. All hydrogen atoms and phen molecules are omitted for clarity.

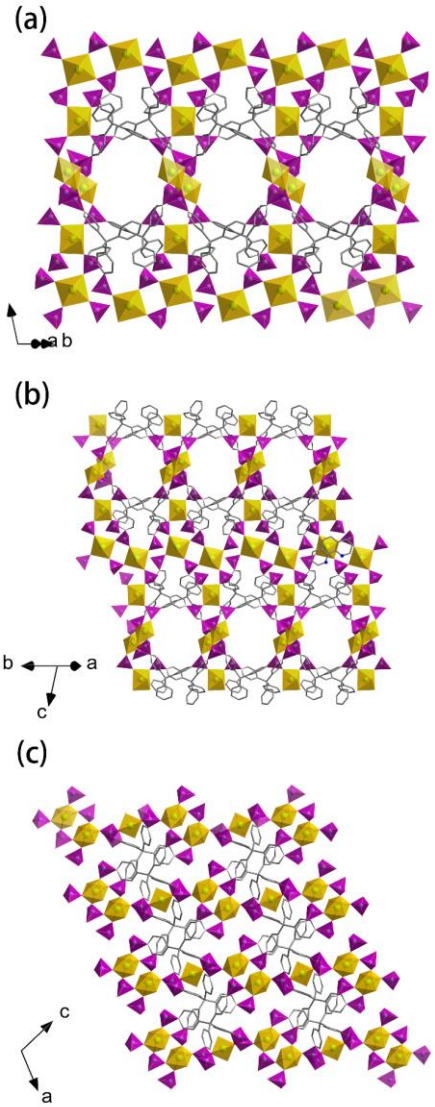

Figure S7. Crystal framework structures of **UPF-114** (a, b, and c), viewed along *a*, *b*, and *c* axis, respectively. UO_6 is represented by the yellow tetragonal bipyramid, while -CPO_3 is represented as a purple tetrahedron, and the guest molecules are omitted for clarity.

UPF-114 crystallizes in the monoclinic space group *C*2/*c*. The asymmetric unit contains one and a half UO_2^{2+} cations, one $TppmH_8$ ligand, and one phen molecule (Fig. S6). $U1O_6$ and $U2O_6$ units adopt tetragonal bipyramid coordination geometry, and four different $TppmH_8$ ligands provide four oxygen atoms in the equatorial plane. The bond lengths of U=O and U-O are in the range of 1.760(4)-1.788(4) Å and 2.243(4)-2.295(4) Å, respectively. One $U1O_6$ and two $U2O_6$ units are connected to give a trimer by corner-sharing of phosphonate groups, acting as 0D-node, further linked by $TppmH_8$, forming a porous 3D-MOF structure. To balance the charge, the protonated phen cations are filled in the space of the structure. **UPF-114** has two kinds of channels that are not crosslinked (Figs. S7a-S7c). The bond lengths of P-O are in the range of 1.494(4)-1.578(4) Å. The bond lengths of P1-O3, P2-O5, P3-O9, and P4-O12 are 1.549(4), 1.567(4), 1.551(4), and 1.578(4) Å, respectively, which belong to P-O-H (Table S4).

1.3 Analysis of Weak Interaction

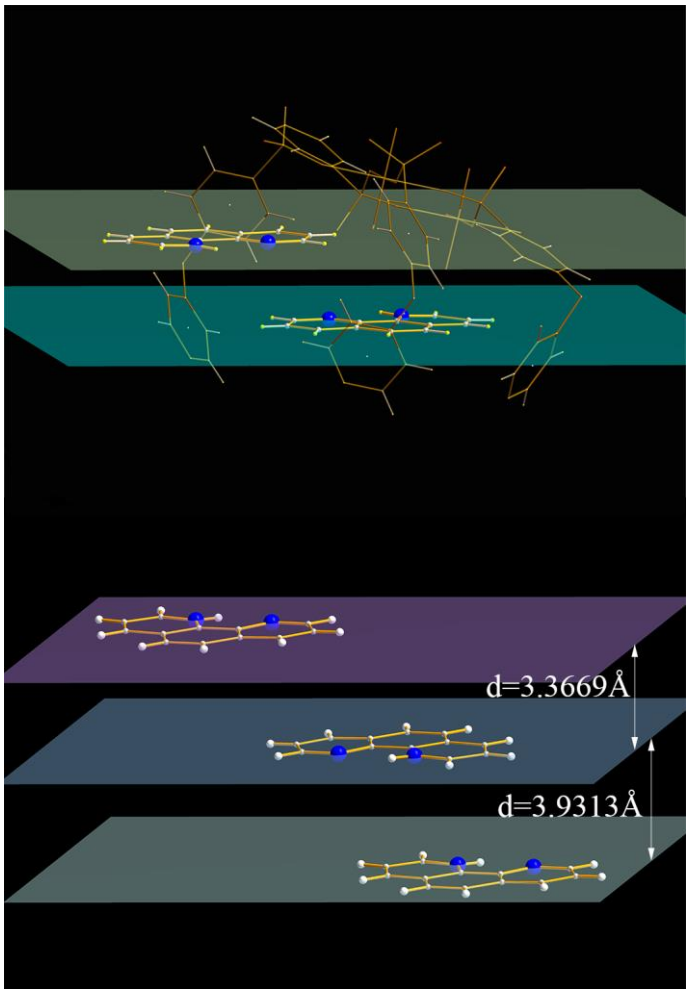

Figure S8. π-π interaction between guest molecules in the framework of **UPF-114**.

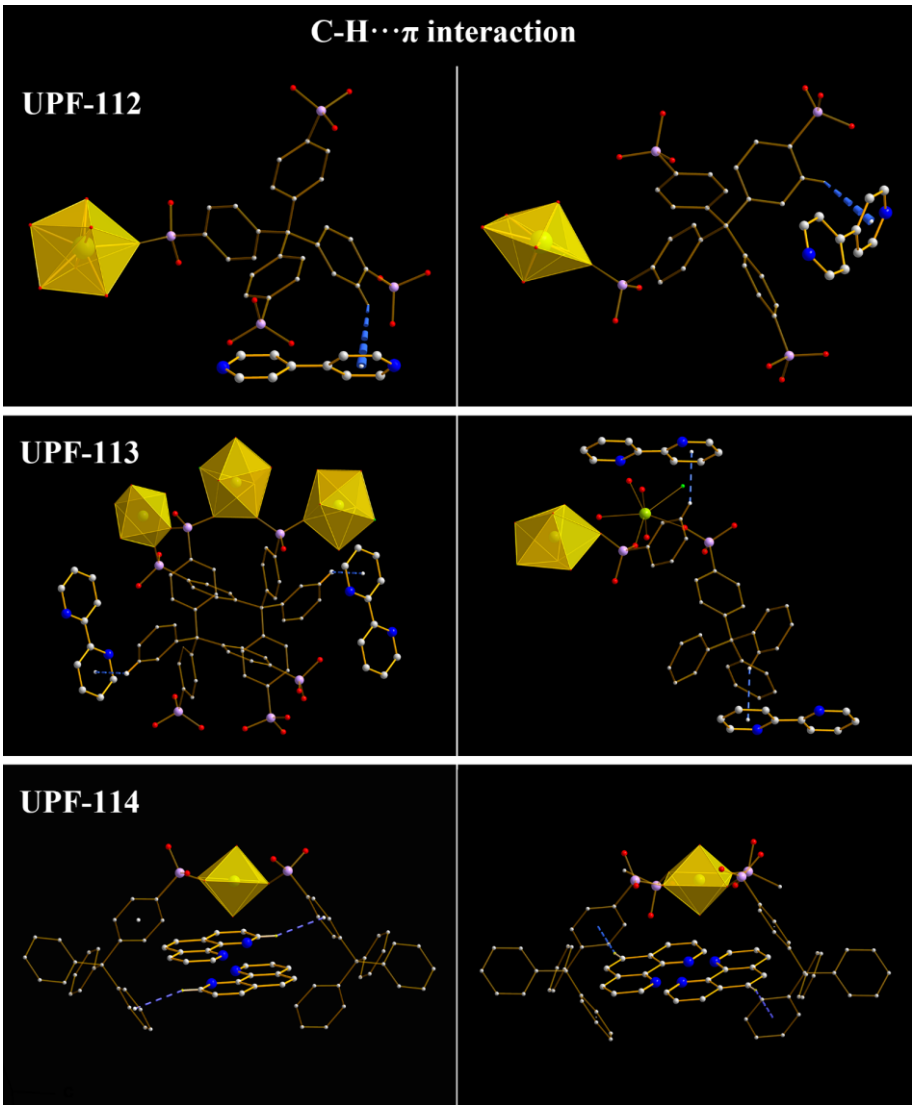

Figure S9. C-H···π interactions (blue dash line) between guest and framework. UO_6 and UO_7 are represented by the yellow tetragonal bipyramid and pentagonal bipyramid, and the hydrogen atoms are omitted for clarity.

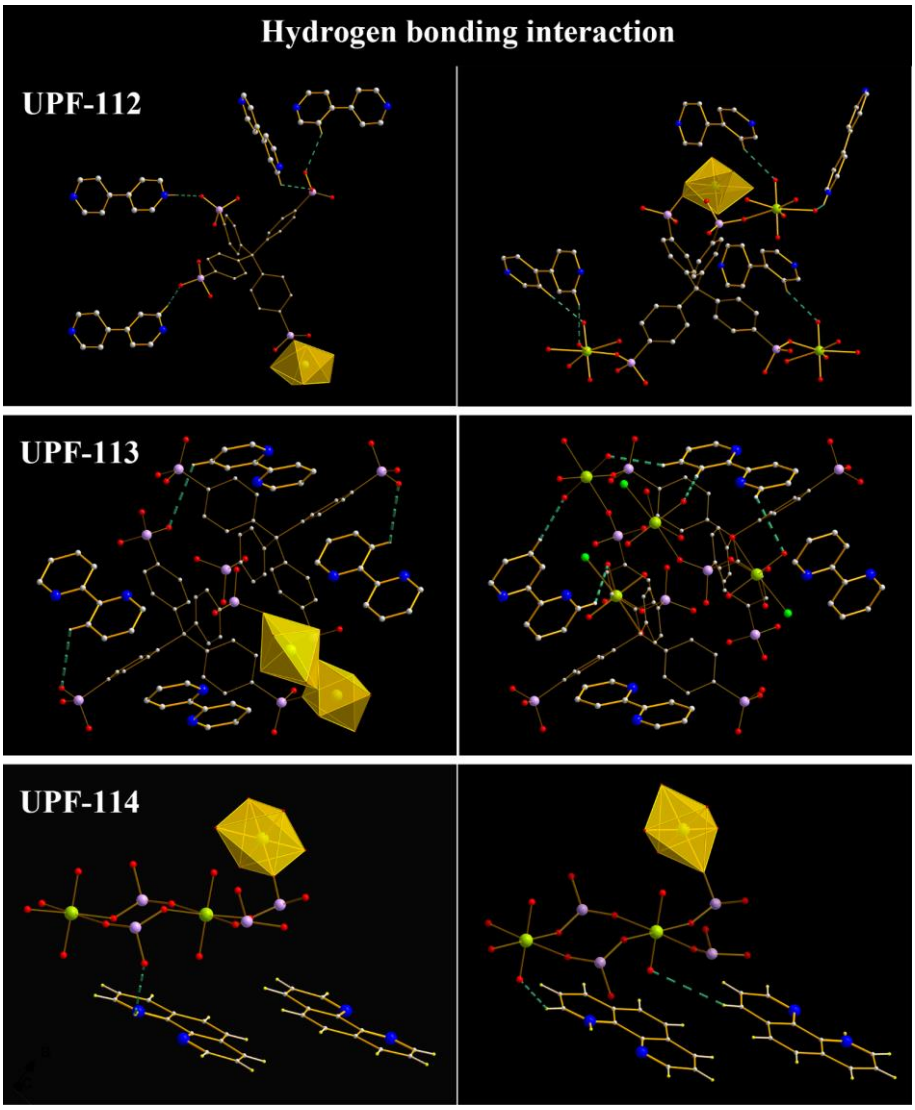

Figure S10. Hydrogen bonding interactions (green dash line) between guest and framework. UO_6 and UO_7 are represented by the yellow tetragonal bipyramid and pentagonal bipyramid, and the hydrogen atoms are omitted for clarity.

Table S5. Bond lengths and bond angles for weak interaction forces between guest molecules and frameworks in **UPF-112**, **UPF-113**, and **UPF-114**.

Species	π-π interaction	C-H···π interactions	hydrogen bonding interaction	
	bond length	bond length	bond length	bond angle
UPF-112		d(H14-π) = 3.1796Å d(H18-π) = 3.1021Å d(H24-π) = 2.8341Å	d(P1-O2···H36) = 2.6170Å	131°
			d(P1-O3···H29) = 2.9000Å	131°
			d(P2-O4···H30) = 2.3305Å	141°
			d(P4-O11···H1-N1) = 1.9397Å	133°
			d(U1-O1w···H26) = 2.7369Å	129°
			d(U1-O13···H34) = 2.5025Å	131°
			d(U1-O12···H3) = 2.8213Å	114°
			d(U1-O14···H32) = 2.8293Å	123°
UPF-113		d(H15-π) = 2.8274Å d(H20-π) = 3.6250Å	d(P4-O12···H27) = 3.7923Å	135°
			d(P1-O3···H33) = 3.4168Å	106°
			d(U2-O14···H28) = 2.4705Å	156°
			d(U3-O10···H30) = 2.7621Å	97°
			d(U3-O16···H32) = 1.9388Å	144°
			d(U3-O14···H33) = 2.7233Å	123°
			d(U3-O15···H35) = 3.0838Å	100°
UPF-114	d_1=3.3669Å d_2=3.9313Å	d(H26-π) = 2.9604Å	d(N2-H2···O8-P) = 3.3631Å	130°
		d(H31-π) = 3.0568Å	d(U2-O14···H37) = 2.3336Å	130°
		d(H35-π) = 3.2510Å	d(U2-O15···H28) = 3.6199Å	100°

1.4 Powder X-ray Diffraction

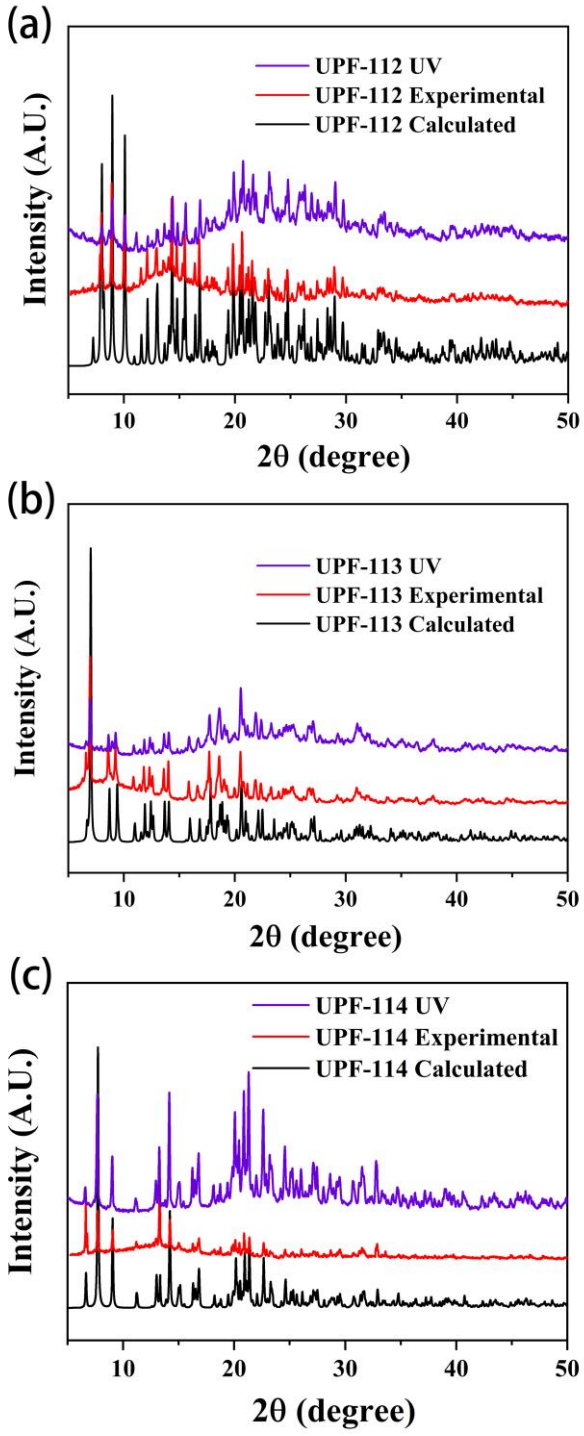

Figure S11. Powder X-ray diffraction (PXRD) patterns of calculated (black), experimental (red) and UV irradiated (violet) for **UPF-112**, **UPF-113** and **UPF-114**.

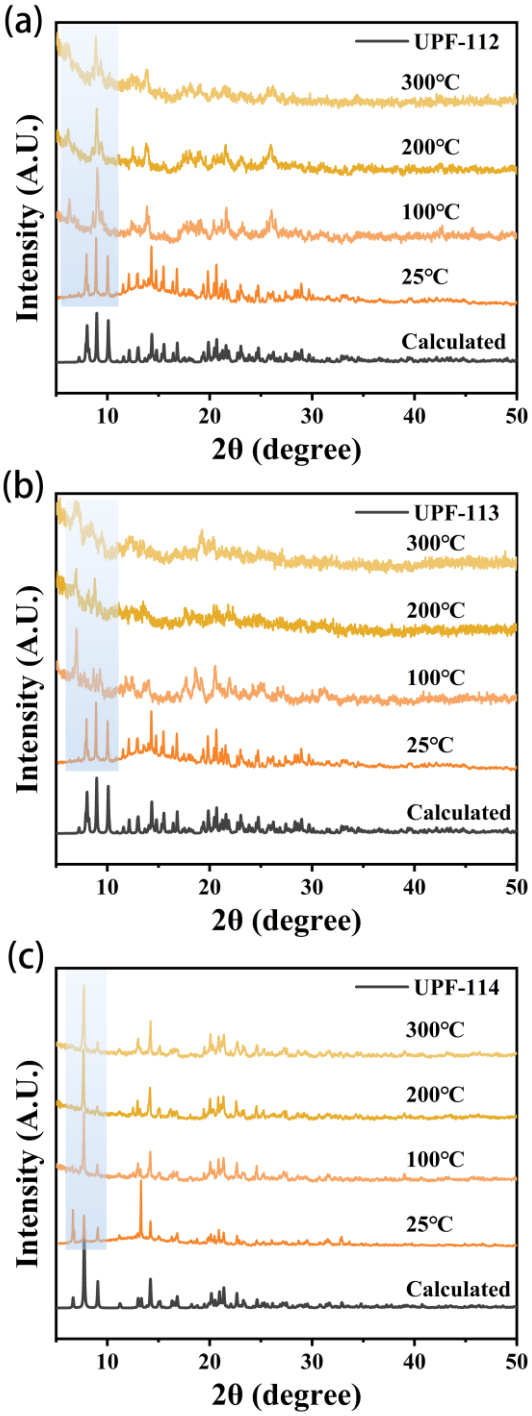

Figure S12. Ex-situ variable temperature powder X-ray diffraction (VT-PXRD) patterns of (a) **UPF-112**, (b) **UPF-113**, and (c) **UPF-114** taken with a Cu Kα radiation source.

1.5 IR and Raman Spectra

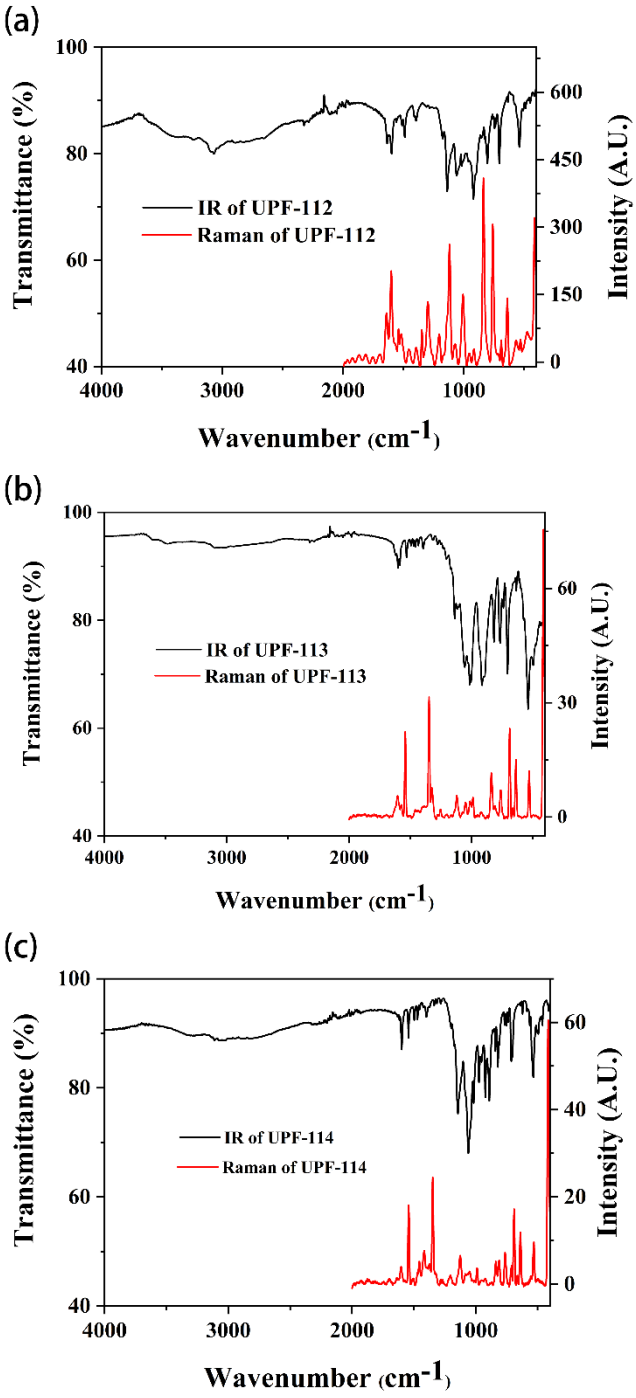

Figure S13. IR and Raman spectra of (a) **UPF-112**, (b) **UPF-113**, (c)**UPF-114**.

1.6 Thermal Gravimetric Analysis

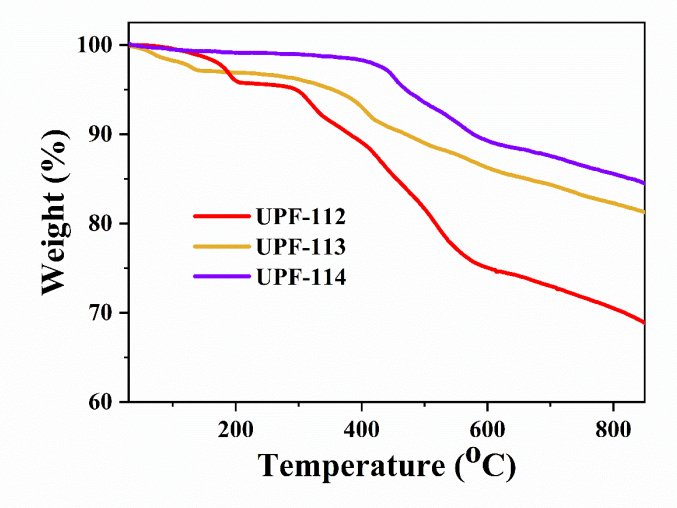

Figure S14. TG patterns of **UPF-112** (red), **UPF-113** (yellow), and **UPF-114** (violet).

UPF-112 started to lose two lattice water molecules and one coordinated water molecule above 120 °C, demonstrating a platform during 200-300 °C. The average weight loss is 4.44 %, similar to a calculated weight loss of 4.52 %. The lattice water molecules of **UPF-113** started to lose with the temperature increase and lost 1.35 % of total weight at 80 °C, similar to the 1.32% calculated by the formula. The aqua ligands of **UPF-113** are removed completely at 135 °C, and the weight loss is 2.72 %, similar to the calculated 2.63 %.

1.7 UV-vis Absorption Spectra

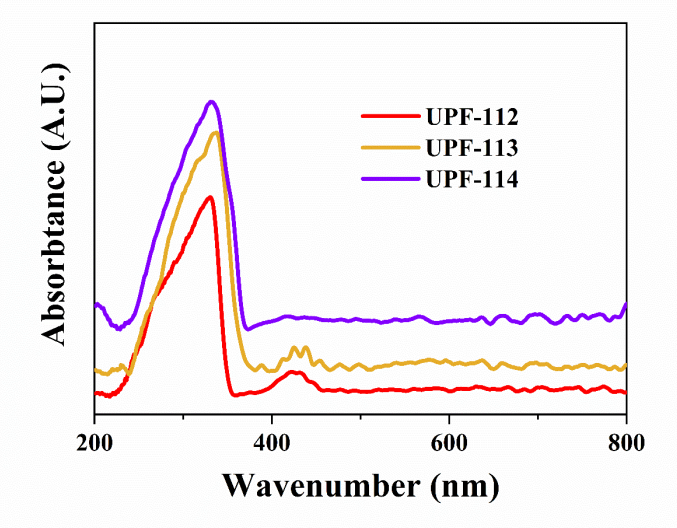

Figure S15. UV-vis absorption spectrum of **UPF-112** (red line), **UPF-113** (yellow line), and **UPF-114** (violet line).

1.8 Photoluminescence Spectra and Fluorescence Quenching Curves

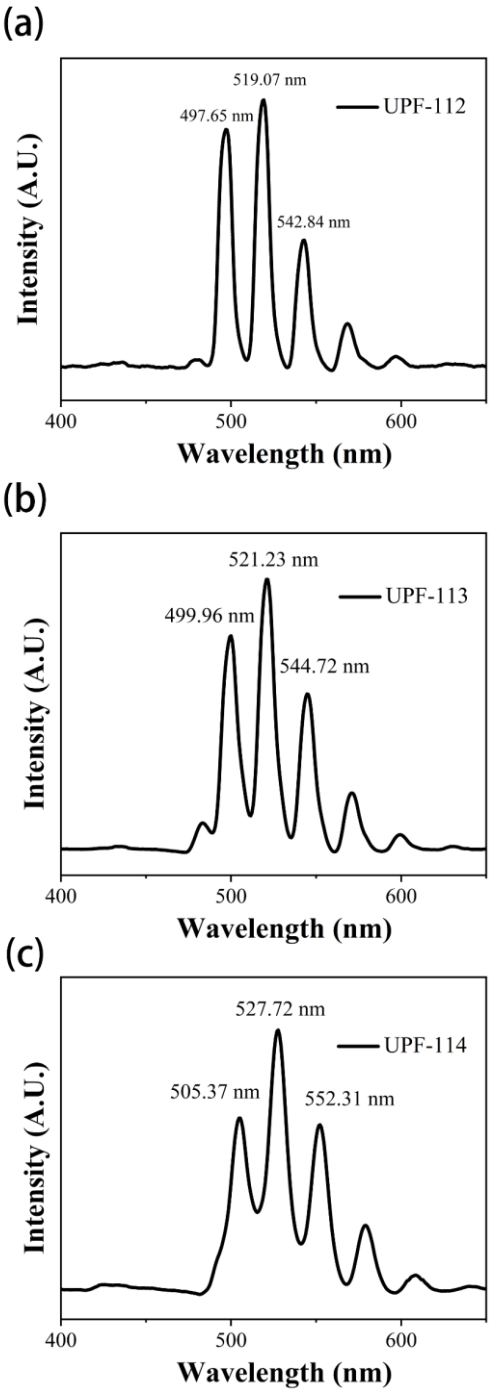

Figure S16. Photoluminescence spectra of **UPF-112**, **UPF-113** and **UPF-114** measured at room temperature.

Table S6. Quenching of **UPF-112** at a peak of 497.65 nm measured at room temperature.

Time (min)	Time (s)	Dosage (mJ)	$(I_0-I)/I_0$ %
0	0	0	0
1	60	2.252×10^{-6}	12.44
3	180	6.755×10^{-6}	24.51
5	300	1.126×10^{-5}	31.80
10	600	2.252×10^{-5}	42.01
20	1200	4.503×10^{-5}	51.76
30	1800	6.755×10^{-5}	57.82
45	2700	1.013×10^{-4}	62.34
60	3600	1.351×10^{-4}	65.67
90	5400	2.026×10^{-4}	69.82
150	9000	3.39×10^{-4}	73.93
180	10800	4.053×10^{-4}	75.42

Table S7. Quenching of **UPF-112** at a peak of 519.07 nm measured at room temperature.

Time (min)	Time (s)	Dosage (mJ)	$(I_0-I)/I_0$ %
0	0	0	0
1	60	2.252×10^{-6}	13.799
3	180	6.755×10^{-6}	26.83
5	300	1.126×10^{-5}	34.24
10	600	2.252×10^{-5}	44.78
20	1200	4.503×10^{-5}	54.69
30	1800	6.755×10^{-5}	60.72
45	2700	1.013×10^{-4}	65.34
60	3600	1.351×10^{-4}	68.42
90	5400	2.026×10^{-4}	72.37
150	9000	3.39×10^{-4}	76.15
180	10800	4.053×10^{-4}	77.46

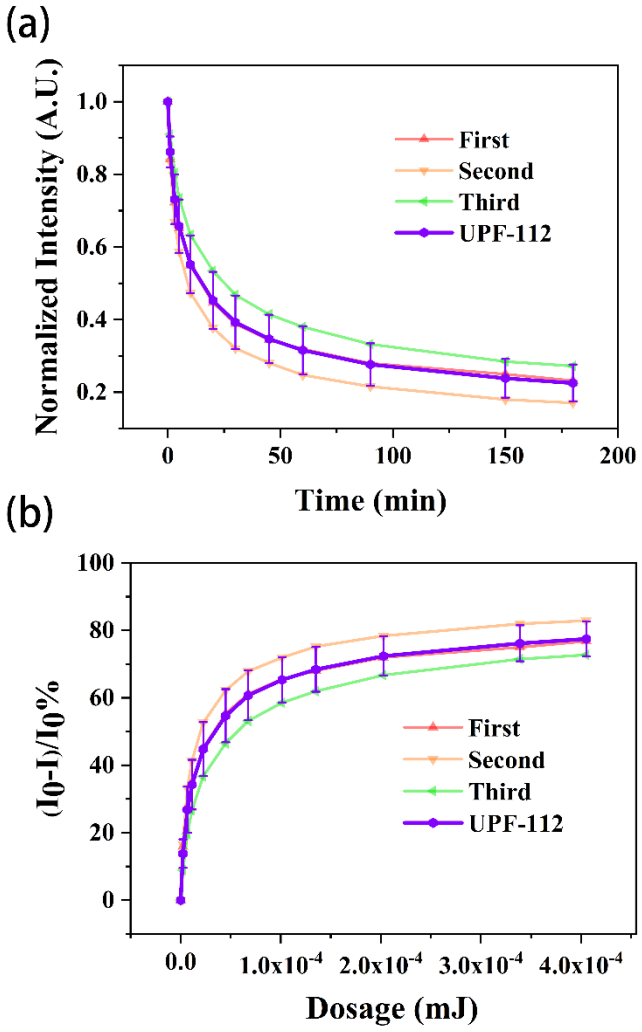

Figure S17. (a) Normalized intensity of **UPF-112** at the peak of 519.07 nm measured at room temperature. (b) Relative fluorescence quenching of **UPF-112** at a peak of 519.07 nm.

Table S8. Quenching of **UPF-112** at a peak of 542.84 nm measured at room temperature.

Time (min)	Time (s)	Dosage (mJ)	$(I_0-I)/I_0$ %
0	0	0	0
1	60	2.252×10^{-6}	14.80
3	180	6.755×10^{-6}	28.39
5	300	1.126×10^{-5}	35.87
10	600	2.252×10^{-5}	46.20
20	1200	4.503×10^{-5}	55.96
30	1800	6.755×10^{-5}	61.74
45	2700	1.013×10^{-4}	66.48
60	3600	1.351×10^{-4}	69.01
90	5400	2.026×10^{-4}	72.71
150	9000	3.39×10^{-4}	76.11
180	10800	4.053×10^{-4}	77.58

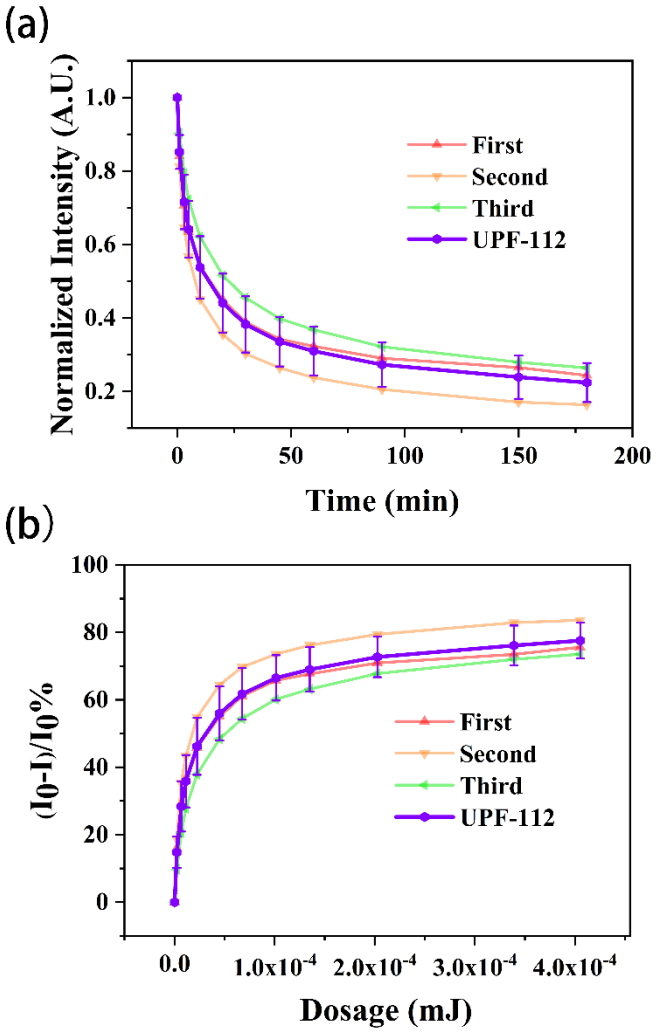

Figure S18. (a) Normalized intensity of **UPF-112** at the peak of 542.84 nm measured at room temperature. (b) Relative fluorescence quenching of **UPF-112** at a peak of 542.84 nm.

Table S9. Quenching of **UPF-113** at a peak of 499.96 nm measured at room temperature.

Time (min)	Time (s)	Dosage (mJ)	$(I_0-I)/I_0$ %
0	0	0	0
1	60	2.252×10^{-6}	18.49
3	180	6.755×10^{-6}	30.93
5	300	1.126×10^{-5}	39.27
10	600	2.252×10^{-5}	50.93
20	1200	4.503×10^{-5}	63.93
30	1800	6.755×10^{-5}	70.80
45	2700	1.013×10^{-4}	77.47
60	3600	1.351×10^{-4}	80.93
90	5400	2.026×10^{-4}	85.96
150	9000	3.39×10^{-4}	88.09
180	10800	4.053×10^{-4}	90.29

Table S10. Quenching of **UPF-113** at a peak of 521.23 nm measured at room temperature.

Time (min)	Time (s)	Dosage (mJ)	$(I_0-I)/I_0$%
0	0	0	0
1	60	2.252×10^{-6}	16.65
3	180	6.755×10^{-6}	29.01
5	300	1.126×10^{-5}	39.57
10	600	2.252×10^{-5}	49.05
20	1200	4.503×10^{-5}	61.69
30	1800	6.755×10^{-5}	67.76
45	2700	1.013×10^{-4}	73.92
60	3600	1.351×10^{-4}	77.96
90	5400	2.026×10^{-4}	82.23
150	9000	3.39×10^{-4}	86.05
180	10800	4.053×10^{-4}	87.34

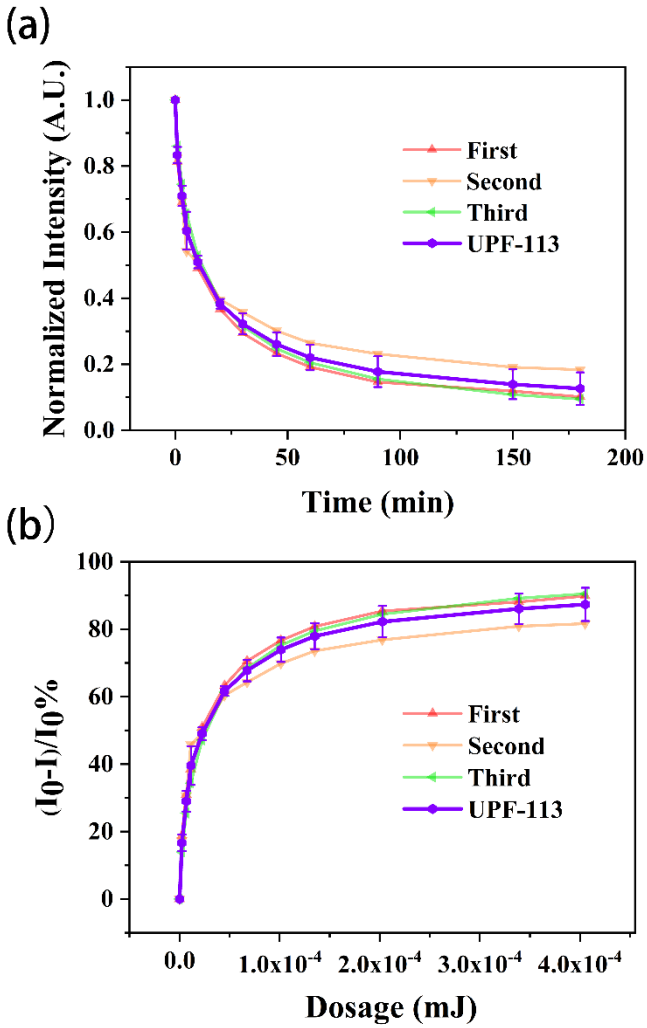

Figure S19. (a) Normalized intensity of **UPF-113** at the peak of 521.23 nm measured at room temperature. (b) Relative fluorescence quenching of **UPF-113** at a peak of 544.72 nm.

Table S11. Quenching of **UPF-113** at a peak of 544.72 nm measured at room temperature.

Time (min)	Time (s)	Dosage (mJ)	$(I_0-I)/I_0$ %
0	0	0	0
1	60	2.252×10^{-6}	16.08
3	180	6.755×10^{-6}	29.05
5	300	1.126×10^{-5}	38.16
10	600	2.252×10^{-5}	47.65
20	1200	4.503×10^{-5}	60.70
30	1800	6.755×10^{-5}	66.25
45	2700	1.013×10^{-4}	72.35
60	3600	1.351×10^{-4}	76.07
90	5400	2.026×10^{-4}	79.49
150	9000	3.39×10^{-4}	82.80
180	10800	4.053×10^{-4}	83.86

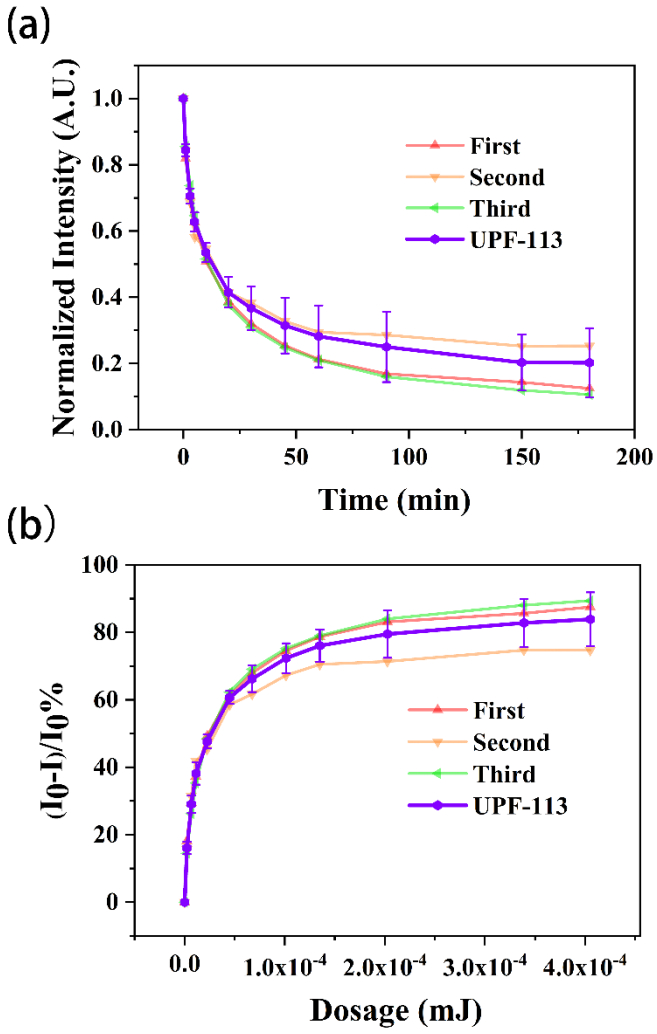

Figure S20. (a) Normalized intensity of **UPF-113** at the peak of 544.72 nm measured at room temperature. (b) Relative fluorescence quenching of **UPF-113** at a peak of 544.72 nm.

Table S12. Quenching of **UPF-114** at a peak of 505.37 nm measured at room temperature.

Time (min)	Time (s)	Dosage (mJ)	$(I_0-I)/I_0$ %
0	0	0	0
1	60	2.252×10^{-6}	33.99
3	180	6.755×10^{-6}	54.14
5	300	1.126×10^{-5}	64.01
10	600	2.252×10^{-5}	75.61
20	1200	4.503×10^{-5}	84.36
30	1800	6.755×10^{-5}	88.10
45	2700	1.013×10^{-4}	91.03
60	3600	1.351×10^{-4}	92.63
90	5400	2.026×10^{-4}	94.46
120	7200	2.701×10^{-4}	95.56

Table S13. Quenching of **UPF-114** at a peak of 527.72 nm measured at room temperature.

Time (min)	Time (s)	Dosage (mJ)	$(I_0-I)/I_0$ %
0	0	0	0
1	60	2.252×10^{-6}	33.97
3	180	6.755×10^{-6}	53.85
5	300	1.126×10^{-5}	64.02
10	600	2.252×10^{-5}	75.53
20	1200	4.503×10^{-5}	84.15
30	1800	6.755×10^{-5}	87.75
45	2700	1.013×10^{-4}	90.85
60	3600	1.351×10^{-4}	92.49
90	5400	2.026×10^{-4}	94.20
120	7200	2.701×10^{-4}	95.48

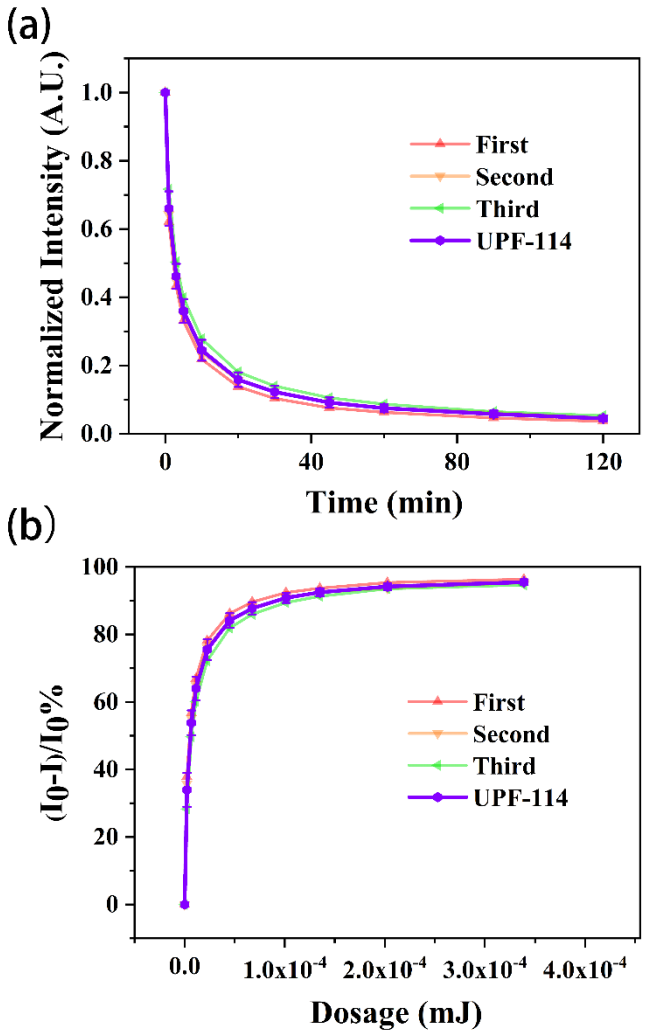

Figure S21. (a) Normalized intensity of **UPF-114** at the peak of 527.72 nm measured at room temperature. (b) Relative fluorescence quenching of **UPF-114** at a peak of 527.72 nm.

Table S14. Quenching of **UPF-114** at a peak of 552.31 nm measured at room temperature.

Time (min)	Time (s)	Dosage (mJ)	$(I_0-I)/I_0$ %
0	0	0	0
1	60	2.252×10^{-6}	33.66
3	180	6.755×10^{-6}	53.65
5	300	1.126×10^{-5}	63.67
10	600	2.252×10^{-5}	75.35
20	1200	4.503×10^{-5}	83.97
30	1800	6.755×10^{-5}	87.58
45	2700	1.013×10^{-4}	90.33
60	3600	1.351×10^{-4}	92.10
90	5400	2.026×10^{-4}	93.87
120	7200	2.701×10^{-4}	95.26

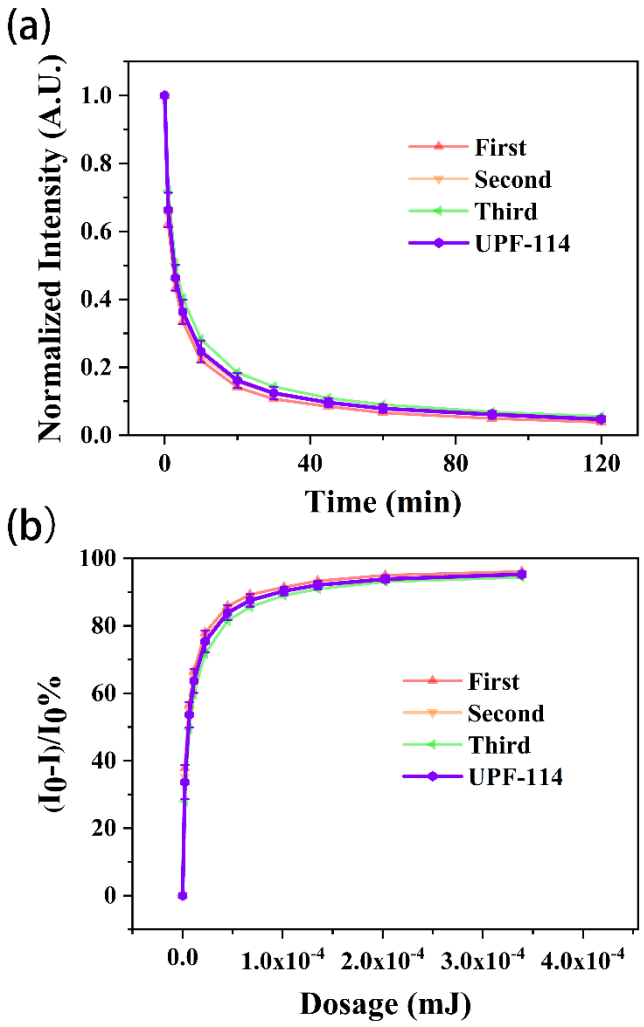

Figure S22. (a) Normalized intensity of **UPF-114** at the peak of 552.31 nm measured at room temperature. (b) Relative fluorescence quenching of **UPF-114** at a peak of 552.31 nm.

1.9 Determination of detection limit

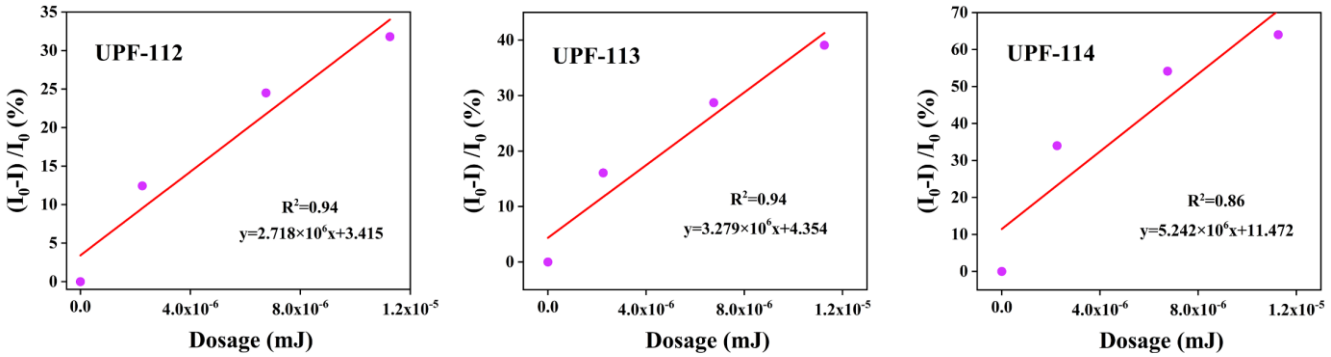

Figure S23. Linear fitting from data points in the low dose range (0 - 1.2×10^{-5} mJ).

Based on the fluorescence measurement shown in Figure S23, the limit of the detection can be determined by the following equations:

$$DT = \frac{3\sigma}{k} \quad (1)$$

$$\sigma = 100 \times \frac{I_{SE}}{I_0} \quad (2)$$

where the detection limit is noted as **DT**; I_{SE} is the standard error of the luminescence intensity (as determined by the baseline measurement of blank samples); I_0 is the measured luminescence intensity; k is the slope obtained from the linear fit in the lower dosage range of the dosage-dependent luminescence intensity calibration curve.[1]

On the basis of the acquired data, the detection limit of **UPF-112** was determined to be 9.54 × 10^{-12} J; the detection limit of **UPF-113** was determined to be 5.98 × 10^{-12} J; the detection limit of **UPF-114** was determined to be 2.96 × 10^{-12} J.

Table S15. Comparison of detection limits of ionizing radiation detectors.

UV-detector	ionizing radiation	intensity decay to half ($T_{1/2}$)	limit of detection (LOD)	Reference
4,4′-di(1H-phenanthro[9,10-d]imidazol-2-yl)-biphenyl (**DPI-BP**)	γ-radiation	\	7 × 10^{-3} Gy	[1]
$(TMA)_2[(UO_2)_4(ox)_4L]$	γ-radiation	\	1.64×10^{-4} Gy	[2]
	X-radiation	\	5.2×10^{-4} Gy	
	UV radiation	20 min	\	
$[UO_2(L)(DMF)]$	UV radiation	\	2.4×10^{-7} J	[3]
$[Hphen]_2[(UO_2)_2(ox)_3$	UV radiation	~ 5 s	6.9 × 10^{-9} J	[4]
$UO_2(ox)(H_2O)\cdot 2H_2O$	X-radiation	\	1.18×10^{-5} Gy	[5]
	γ-radiation	\	1.42×10^{-5} Gy	
	UV radiation	~112 s	\	
Ln-DBTPA	UV radiation	\	9.1 × 10^{-9} J	[6]
$[4,4\text{-bpyH}]_{1.5}(UO_2)(TppmH_{4.5})(H_2O)\cdot 2H_2O$ (**UPF-112**)	UV radiation	19 min	9.54 × 10^{-12} J	This work
$[2,2\text{-bpyH}](UO_2)_2(TppmH_3)(H_2O)\cdot H_2O$ (**UPF-113**)	UV radiation	12 min	5.98 × 10^{-12} J	
$[phenH](UO_2)_{1.5}(TppmH_4)$ (**UPF-114**)	UV radiation	3 min	2.96 × 10^{-12} J	

1.10 EPR Spectra Before and After UV Irradiation

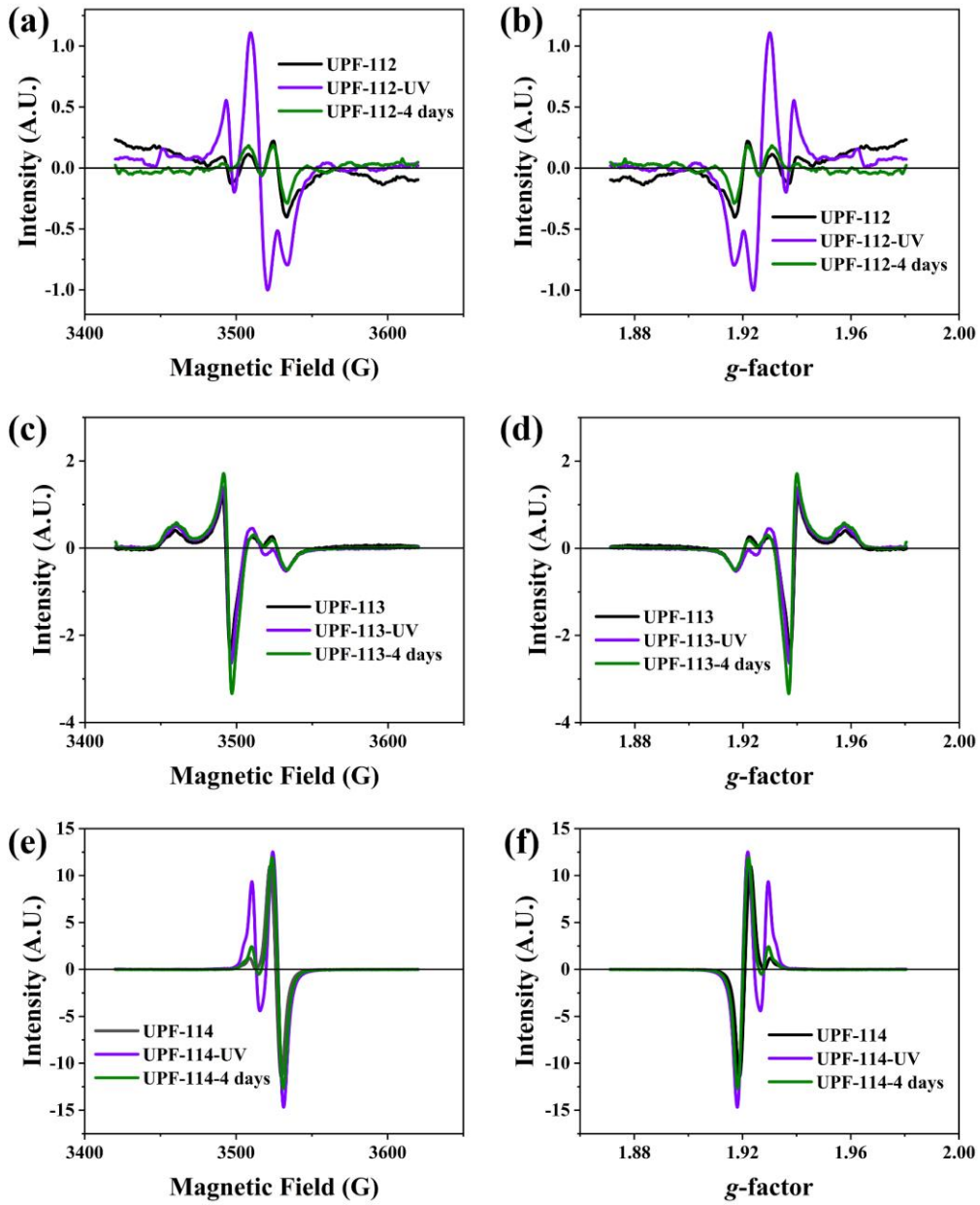

Figure S24. EPR spectra of **UPF-112** (a, b), **UPF-113** (c, d), and **UPF-114** (e, f) before and after UV irradiation for 3 hours and storied in the dark for 4 days.

2. References

1. J.-M. Han, M. Xu, B. Wang, N. Wu, X. Yang, H. Yang, B. J. Salter and L. Zang, Low Dose Detection of γ Radiation via Solvent Assisted Fluorescence Quenching, *J. Am. Chem. Soc.*, 2014, **136**, 5090-5096.
2. J. Xie, Y. Wang, W. Liu, X. Yin, L. Chen, Y. Zou, J. Diwu, Z. Chai, T. E. Albrecht-Schmitt, G. Liu and S. Wang, Highly Sensitive Detection of Ionizing Radiations by a Photoluminescent Uranyl Organic Framework, *Angew. Chem. Int. Ed.*, 2017, **56**, 7500-7504.
3. W. Liu, X. Dai, J. Xie, M. A. Silver, D. Zhang, Y. Wang, Y. Cai, J. Diwu, J. Wang, R. Zhou, Z. Chai and S. Wang, Highly Sensitive Detection of UV Radiation Using a Uranium Coordination Polymer, *ACS Appl. Mater. Interfaces*, 2018, **10**, 4844-4850.
4. J. Xie, Y. Wang, D. Zhang, C. Liang, W. Liu, Y. Chong, X. Yin, Y. Zhang, D. Gui, L. Chen, W. Tong, Z. Liu, J. Diwu, Z. Chai and S. Wang, Photo-exfoliation of a highly photo-responsive two-dimensional metal–organic framework, *Chem. Commun.*, 2019, **55**, 11715-11718.
5. J. Xie, Y. Wang, W. Liu, C. Liang, Y. Zhang, L. Chen, D. Sheng, Z. Chai and S. Wang, A uranyl based coordination polymer showing response to low-dosage ionizing radiations down to 10−5 Gy, *Sci. China: Chem.*, 2020, **63**, 1608-1612.
6. S. Zhang, L. Chen, J. Xie, Y. Zhang, F. Huang, X. Wang, K. Li, F. Zhai, Q. Yang, L. Chen, Y. Wang, X. Dai, Z. Chai and S. Wang, Turn-up Luminescent Sensing of Ultraviolet Radiation by Lanthanide Metal–Organic Frameworks, *Inorg. Chem.*, 2022, **61**, 4561-4565.